Measurements of flow around inclined jets by stereoscopic PIV

T. Nishimura*, S. Inaba*, K. Hishida*, M. Maeda*

*Department of System Design Engineering,
Keio University, 3-14-1 Hiyoshi, Kohoku-ku, Yokohama 223-8522, Japan

Key Words: Stereo PIV, three-dimensional measurement, inclined jet, applicability study

Abstract

A stereo PIV (SPIV) acquisition and analysis system was developed to obtain three velocity components in flow fields. The software features a third order mapping function method. The system was calibrated by imaging a square grid in five measurement planes with two Kodak Megaplus cameras oriented at 30 ° with respect to the bisector between them. The captured images were transformed into real coordinates by employing a set of transform matrices computed for each calibration plane. The SPIV system was tested on a two-dimensional oblique jet with a Reynolds number of 1800. Three-dimensional data were taken in a vertical (x, y) plane, parallel to the jet span. The SPIV results were compared with LDV data and two-dimensional PIV data obtained in the vertical (y, z) plane of a similar jet. The SPIV measurements yielded accurate values for the in-plane and out-of-plane mean velocity components. The in-plane rms component was also in agreement. The measured out-of-plane rms component was accurate in part of the field, but overestimated in another part due to a decrease of the resolution in rms error. By improving the calibration procedure the out-of-plane errors can be minimized.

Moreover the system was applied to three-dimensional jet-to-cross flow (**Figure 1 a)**). Examples of a three SPIV vector map taken in sequence are shown in **Figure 1 b)**. Three-dimensional vorticity iso-surfaces were successfully reconstructed from temporal series of velocity in a cross-section at plane.

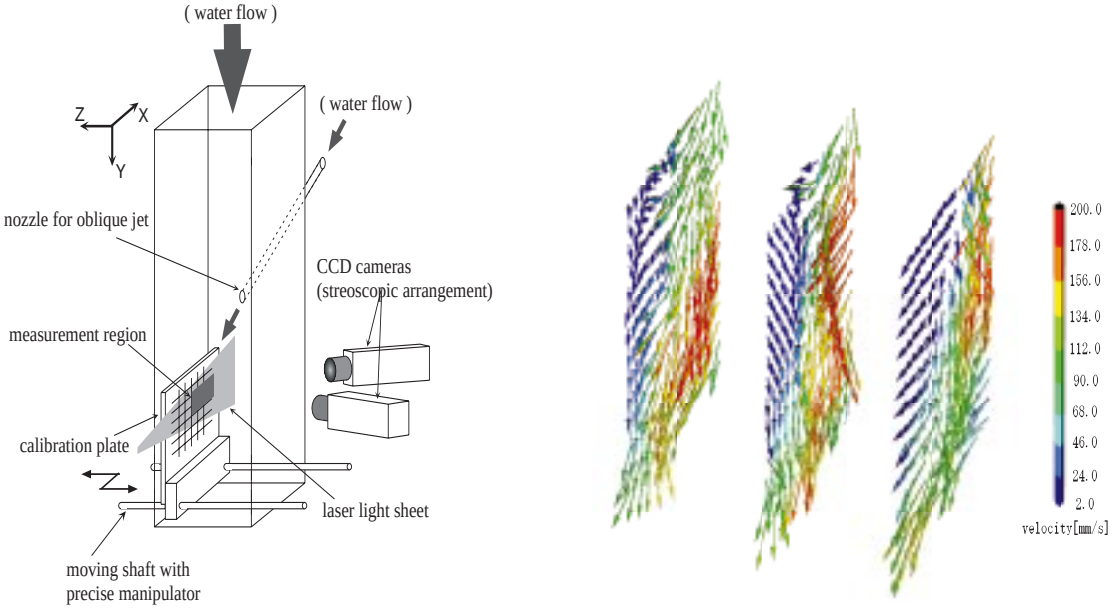

a) Injected round jet in channel flow **b)** Three-component velocity vectors

Figure 1 SPIV set-up

1 Introduction

The aquisition of three-dimensional information in flow fields is quite important in order to construct models for numerical simulations and to comprehend three-dimensional phenomena. The two-dimensional approach, namely Particle Image Velocimetry (PIV)[1], has already been put into practical use.

A stereoscopic PIV (SPIV) system is capable of measuring all three velocity components within small zones of a planar domain. Two types of implementaion for SPIV have been reported. A 'non-calibration method' was demonstrated by Prasad and Adrian (1993)[2]. The method employs input parameters specific to the particular experiment, such as the refractive indices of fluid and container and measured dimensions between cameras and the 'image' region. The method also employs imaging optics with strict specification (minimal aberration) to reconstruct three-component vectors without calibration. In contrast, Willert (1997)[5] and Soloff, Adrian, and Liu (1997)[3] discuss 'mapping function methods' that determine the mapping function by *in-situ* calibration. The mapping functions determined by this method are contained within matrices that transform the pixel coordinate systems aligned with the cameras into real coordinate systems aligned with the image plane. In this case, quantities such as refractive index need not be measured precisely, and optical aberrations do not introduce systematic errors.

In this paper, we describe a 'mapping function' SPIV system developed at Keio University[11]. The mapping algorithms were calibrated and assessed by comparison with direct measurements of displacement. The system was tested in experimentally using a steady two-dimensional flow. The SPIV results were compared with results from LDV and from a standard two-dimensinal PIV method oriented prependicular to the stereo measurement plane.

The reliability of the system was confirmed and it was employed for a jet flow from the side wall in a channel, a configuration which is often used for mixing, cooling etc. While the flow arround the jet was not so clear even the combination of simple flows, ie. main flow with impinging jet makes a strongly fluctuating flow behind the jet, downstream of the main flow. The SPIV system was also employed in the challenging task of measuring three-dimensional flows.

2 Image reconstruction method and recombination procedure

The mapping function is a matrix as follows,

$$\underbrace{\begin{pmatrix} x_1 & y_1 \\ x_2 & y_2 \\ \vdots & \vdots \\ x_{16} & y_{16} \\ \vdots & \vdots \\ x_n & y_n \end{pmatrix}}_{\boldsymbol{x}} = \underbrace{\begin{pmatrix} 1 & X_1 & {X_1}^2 & {X_1}^3 & X_1Y_1 & \dots & {X_1}^3{Y_1}^3 & Y_1 & {Y_1}^2 & {Y_1}^3 \\ 1 & X_2 & {X_2}^2 & {X_2}^3 & X_2Y_2 & \dots & {X_2}^3{Y_2}^3 & Y_2 & {Y_2}^2 & {Y_2}^3 \\ \vdots & \vdots & & & & \ddots & & \vdots & \vdots & \\ 1 & X_{16} & {X_{16}}^2 & {X_{16}}^3 & X_{16}Y_{16} & \dots & {X_{16}}^3{Y_{16}}^3 & Y_{16} & {Y_{16}}^2 & {Y_{16}}^3 \\ \vdots & \vdots & & & & \ddots & & \vdots & \vdots & \\ 1 & X_n & {X_n}^2 & {X_n}^3 & X_nY_n & \dots & {X_n}^3{Y_n}^3 & Y_n & {Y_n}^2 & {Y_n}^3 \end{pmatrix}}_{\boldsymbol{X}} \underbrace{\begin{pmatrix} a_1 & b_1 \\ a_2 & b_2 \\ \vdots & \vdots \\ a_{16} & b_{16} \end{pmatrix}}_{\boldsymbol{A}} \tag{1}$$

Where $\boldsymbol{x}$ and $\boldsymbol{X}$ are matrices which have positions of planar x, y in real and pixel coordinate systems, and the elements x_i, y_i, X_i, Y_i are determined by calibration process. $\boldsymbol{A}$ is the coefficient transformation matrix. $\boldsymbol{A}$ is determined by using the least square method from the calibrated $\boldsymbol{x}$ and $\boldsymbol{X}$ which is shown in the following equation. ($\boldsymbol{x}$ and $\boldsymbol{X}$ are over-determinant matrices.)

$$\boldsymbol{A} = (\boldsymbol{x}^T \boldsymbol{X})^{-1} \boldsymbol{X}^T \boldsymbol{x} \tag{2}$$

The transformation matrix $\boldsymbol{A}$ makes transformation between a particular plane in real coordinates and a pixel (planar) coordinate system possible. In the SPIV system, it is that 18 transform matrices at several z postions are required to determine three-dimensional real coordinates (**Figure 2**). In the case of the three-plane calibration procedure, a total of six transform matrices are calculated for a given calibration plate at specific z position. In the case of the five-plane calibration procedure, a total of ten matrices are calculated.

A 'recombination procedure' as shown in **Figure 3** reconstructs a three-component vector from a pair of recorded two-dimensional vectors. The corresponding two-dimensional vectors in each camera have to be chosen, and the position of the three-component vector has to be determined. When a vector is recorded in one camera, a position of the vector can be transformed into real coordinate, thus the origin of the vector in real coordinates is determined. The origin of the vector in real coordinates can also be transformed into anothor camera coordinate, and the corresponding individual vectors on each CCD image can be combined.

In the case of the three-plane calibration procedure, a head of the two-dimensional vector recorded on the image plane determines two points in real coordinates by transformation. In the five-plane calibration procedure, four points are determined. A line may be determined, if two points exist, but the line is determined using the least squares method with four points in such a case. Thus, two lines in real coordinates are determined by a pair of vectors.

The intersection of the lines determines the true three-component vector. However, the lines do not intersect in most cases due to the error occuring in two-dimensional vectors, thus the least squares method might be employed to determine the intersection of the lines due to its over-determination of the matrices. It is equivalent to finding the midpoint of least distance between lines.

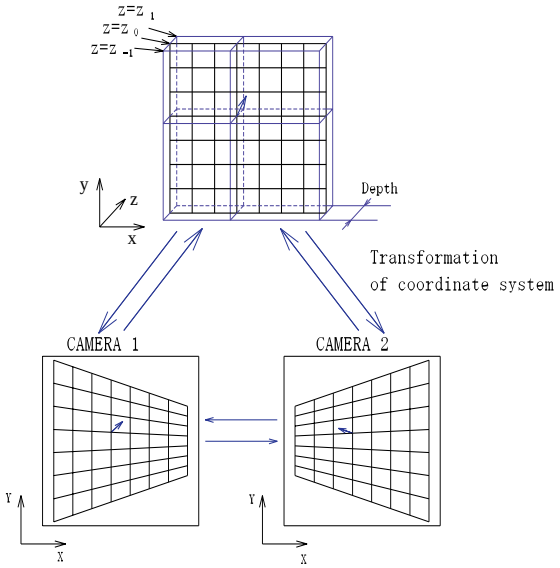

Figure 2 Transformation between pixel and real coordinate planes

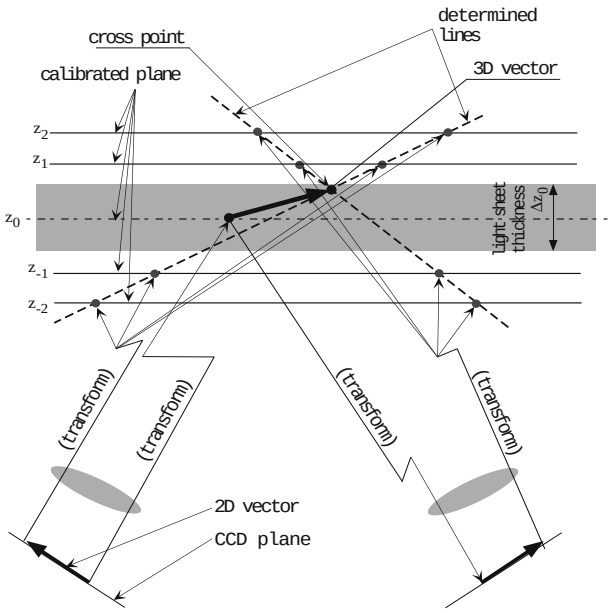

Figure 3 Reconbimation procedure to form three-component vectors

3 Jet Flow Experiment

3.1 Applicability study of the system using an oblique plane jet

Figure 4 a) shows the experimental set-up for two-dimensional slanted jet measurement. The experiments were performed in a vertical Plexiglas water tank with dimensions 100 mm × 100 mm × 400 mm that was connected to a closed-loop flow circuit. The size of measurement region was 40 mm × 40 mm. Mean velocity at the spouting point was 60mm/s ($R_e = 1800$), width of the nozzle was 30 mm, and the slant angle was 30°. The waterflow was seeded with neutrally buoyant polystyrene particles with diameter ranging from 3-30 μm. The slanted jet flow is illuminated by two frequency-doubled Nd:YAG lasers. The thickness of each sheet was 2 mm. Two Kodak Megaplus cameras (1008 × 1018 pixels, 8bit) were set in a Scheimpflug configuration[5]. To calibrate the SPIV system, a calibration plate with grid was set up inside of the flow tank. The plate position was controlled with a precision manipulator. The plate and traversing system were removed from the flow field before the measurements were taken.

For comparison, a two-dimensinal 'classical' PIV mesurement technique was applied in vertical planes normal with the jet span. **Figure 5** shows a side view of the velocity field of the slanted jet and SPIV measuring section. The origin, $y = 0$, is located at 10 mm downstream of the center of the nozzle exit plane. In all PIV and SPIV measurements, the illumination interval of the laser pulses was 10 ms. Interrogation windows were 20 pixels on a side corresponding to 0.91 mm.

LDV measurements were carried out to compare time-averaged corresponding 'point' velocities in the spanwise (y) and normal (z) directions. The beam crossing angle was 9.2 ° yeilding a measuring volume of 0.12 mm × 0.12 mm × 1.5 mm. The FFT resolution of the frequency was 0.031 kHz, and 0.12 mm/s was the resolution of velocity.

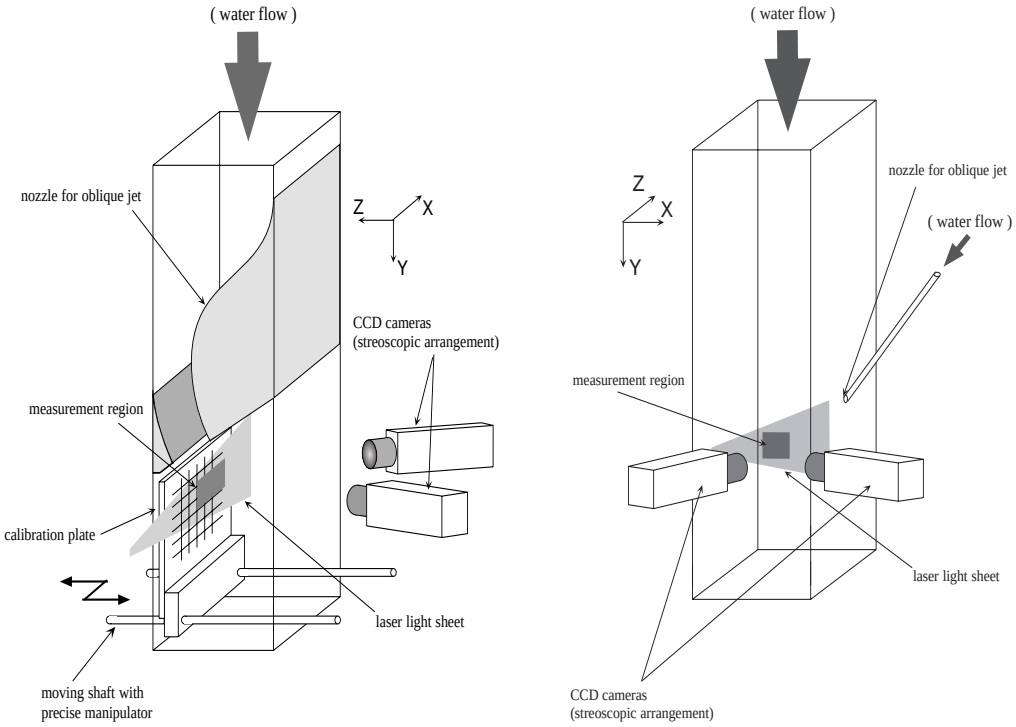

a) Oblique plane jet **b)** Injected round jet in channel flow

Figure 4 Jet flow facility and SPIV set-up

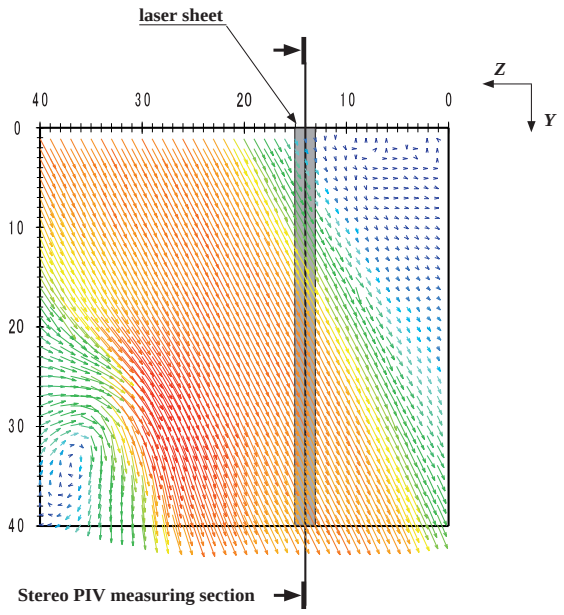

Figure 5 Instantaneous velocity field obtained by two-dimensional PIV

3.2 Injected round jet in channel flow

Figure 4 b) illustrates the experimental set-up for a three-dimensional slanted round jet. The test section is a 400-mm-long vertical channel having square cross section of 100 mm × 100 mm that was connected to a closed-loop flow circuit. The size of the obseving area was 40 mm × 40 mm. The mean cross-flow velocity in the channel was 20 mm/s and using the equivalent hydrodynamic diameter of the channel as a reference length $R_e = 1000$. The mean jet-flow velocity was 200 mm/s with a flow angle of 45° . The diameter of the nozzle was 4 mm. The resulting jet Reynolds number was 800. The jet-to-cross flow velocity ratio ($R = U_{\text{jet}}/U_{\text{channel}}$) in the present experiment is 10. The time between laser pulses was 3 ms. Other parameters and configuration of the set-up were the same as in the oblique plane jet experiment.

4 Results and discussion

4.1 Applicability study of the system using an oblique plane jet

The velocities at 0 mm $\leq y \leq$ 36 mm were measured by SPIV to compare with those by two-dimensional PIV and LDV. The symbol **Stereo3_4.0** in **Figures 6-8** indicates the SPIV measurement by three-plane calibration procedure; three measurement planes placed at 0 mm and ±4.0 mm were used to determine the appropriate transform matrices. Similarly the symbol **Stereo5_0.2_0.5** in **Figures 6-8** indicates the five-plane calibration procedure with planes, located at 0 mm, ±0.2 mm and ±0.5 mm.

The mean and rms velocities were obtained by ensemble averages of both classical and stereo PIV measurements and the results are plotted in **Figure 6** and **Figure 7**. The PIV measurenents are compared with LDV measurements taken separately.

The plots of mean velocity in **Figure 6** show that the SPIV measurements closely coincided with the classical PIV and LDV measurements in the y-direction over the full range in the vertical position. Likewise, the mean results in velocities of SPIV calibrated by three-plane procedure in the z-direction closely agreed with the classical PIV and LDV when the z-displacements between each calibration plane were small, while the error was strongly reduced in the five-plane case.

In **Figure 7**, the rms value vertical component (v) is similar to that of the LDV and SPIV across the range examined. The values for classical PIV are large where the velocity gradient appears. The classical PIV uses a single camera whose axis is perpendicular to the illuminated plane in order to obtain in-plane velocity components. Due to the in-plane recording, the technique only recovers the projection of the vector. For this reason, these values included perspective error. For evaluation of rms values in the z-direction, a larger z-displacement of the plate was required in the three-plane calibration procedure, while the z-displacement was significant for evaluation of mean velocities in the three-plane calibration case. There was a limitation in the accuracy of the measured fluctuation toward the edge of the view area (at larger y). The limitation was caused by a decrease of the resolution due to the angle between each camera and the line perpendicular to the measurement plane. In this case, the error could be also minimized using the calibration procedure by five planes. The SPIV system can be well applied to the flow field under relatively lager fluctuations (0 mm $\leq y \leq$ 10 mm).

Figure 8 shows PDF of the v- and w- velocity components at the velocity gradient ($y = 5$ mm). The results illustrated that the unavoidable error in the classical two-dimensional PIV method could be reduced significantly using the SPIV method.

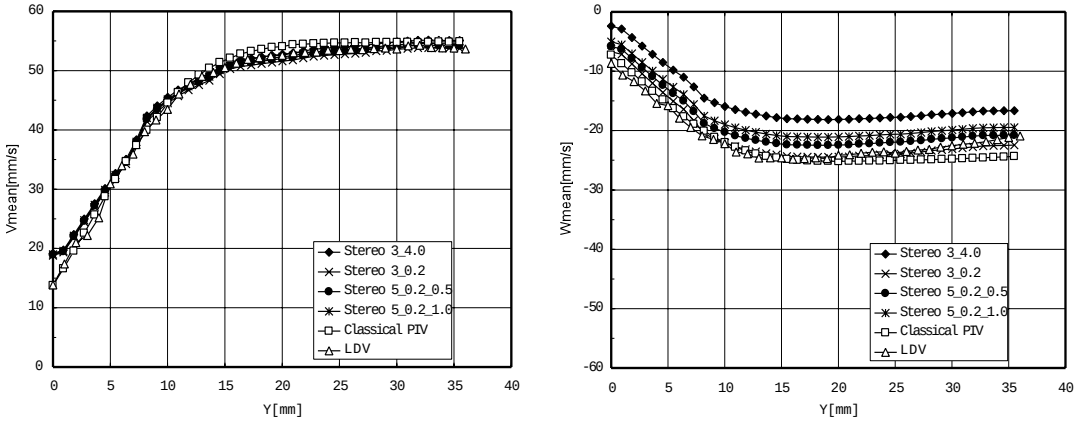

a) Streamwise direction **b)** Normal direction

Figuere 6 Ensemble-average mean velocities

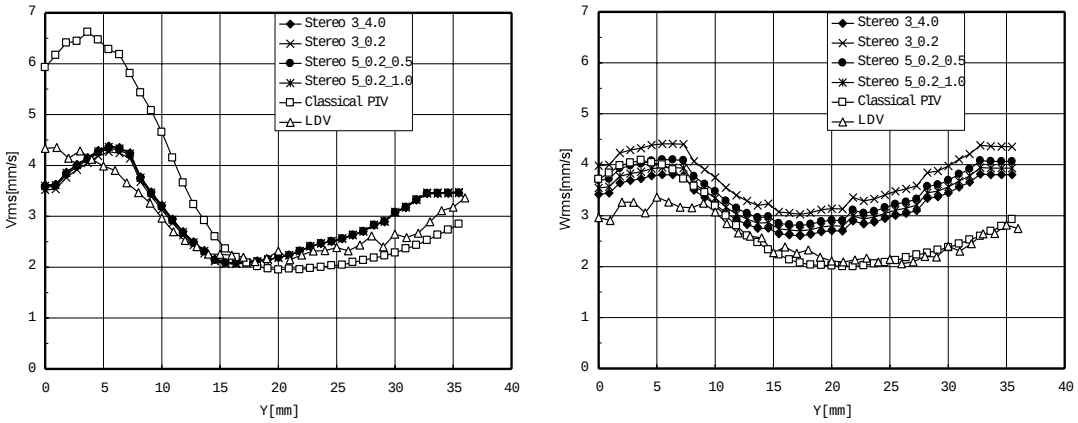

a) Streamwise direction **b)** Normal direction

Figure 7 Ensemble-average rms velocities

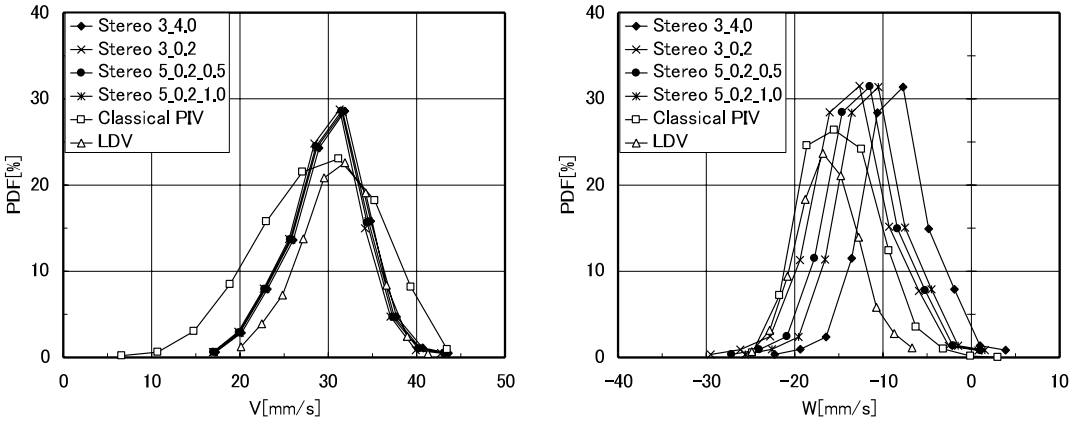

a) Streamwise direction **b)** Normal direction

Figure 8 Probably Density Function of velocity (y=5 [mm])

4.2 Injected round jet in channel flow

In the present experiment, five calibration planes spaced at ±0.2 mm and ±10mm apart from the middle plane, were employed to obtain the transform matrices. **Figure 9 a)** displays a time-averaged mean three-component vector map with contour levels corresponding to values of the w-velocity component. The nozzle exit is located at the right hand side and the jet blows from the upper side slanted downstream to the left (see **Figure 4 b)**), where the z-axis was fixed at the center of the nozzle. This field indicates a strong third component of the jet flow of the nozzle exit from the side wall and the third component in downstream becomes weaker. The z-position of **Figure 9 b)** has been shifted 3 mm from the center of the nozzle. This field indicates that the jet causes uniformities extending into the flow. There were significant change between each field in the flow.

Examples of a five SPIV vector map taken in sequence are shown in **Figure 10**. The time between plots is $dt = 0.067$ seconds, and the measuring plane was the same as **Figure 9 a)**. The jet discharging into a cross flow creates a complex flow field. These kinds of fields show in fact that three-component velocity vectors were observed and indicated that the jet flow makes a periodic fluctuation in the shear layer.

To estimate three-dimensional vortical structure, spatial stretch in the z-direction which could not be measured even by SPIV, was assumed as equivarent to time direction and $dz = dtU_{\mathrm{jet}}/2$. Each component of the vorticity defined in this way is computed as follows,

$$\omega_x = \frac{dw}{dy} - \frac{dv}{dz}, \quad \omega_y = \frac{du}{dz} - \frac{dw}{dx}, \quad \omega_z = \frac{dv}{dx} - \frac{du}{dy} \tag{3}$$

A typical example of vorticity iso-surfaces in two parallel measured planes are shown in **Figures 11-13** ($|\omega| = 0.4|\omega_{\max}|$). Distance between each layer was 3mm, and each measurement was taken separately. Most of the vorticity is concentrated in the jet shear layers. **Figures 11 a)-13 a)** results from **Figure 9 a)**. **Figures 11 b)-13 b)** also was derived using **Figure 9 b)**. Three-dimensional vorticity iso-surfaces were successfully reconstructed from temporal series of velocity in a cross-section at plane. To obtain three-dimensional volumetric data from SPIV data, 35 image pairs were used. The time scale was 2.33 seconds. Variation in the vorticity iso-surface in the z-direction were clearly observed. This was considered to be caused by three-dimensional vortical structure. When the origin of the z-axis was located at the center of the nozzle exit plane, larger vortical structures in the shear layer were reduced through mixing to downstream. When the z-position of measuring plane was shifted 3 mm from the center of the nozzle, periodic vortical structures resulting from the jet extending in the z-direction was observed.

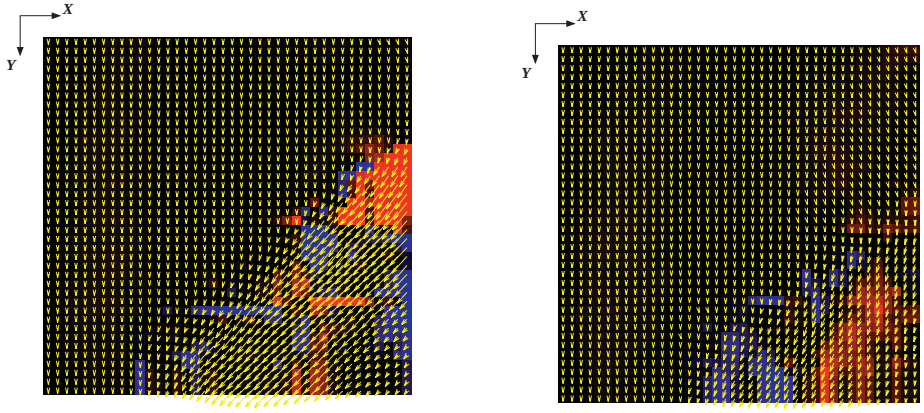

a) z=0 [mm] **b)** z=3 [mm]

Figure 9 Mean three-component velocity fields obtained by SPIV

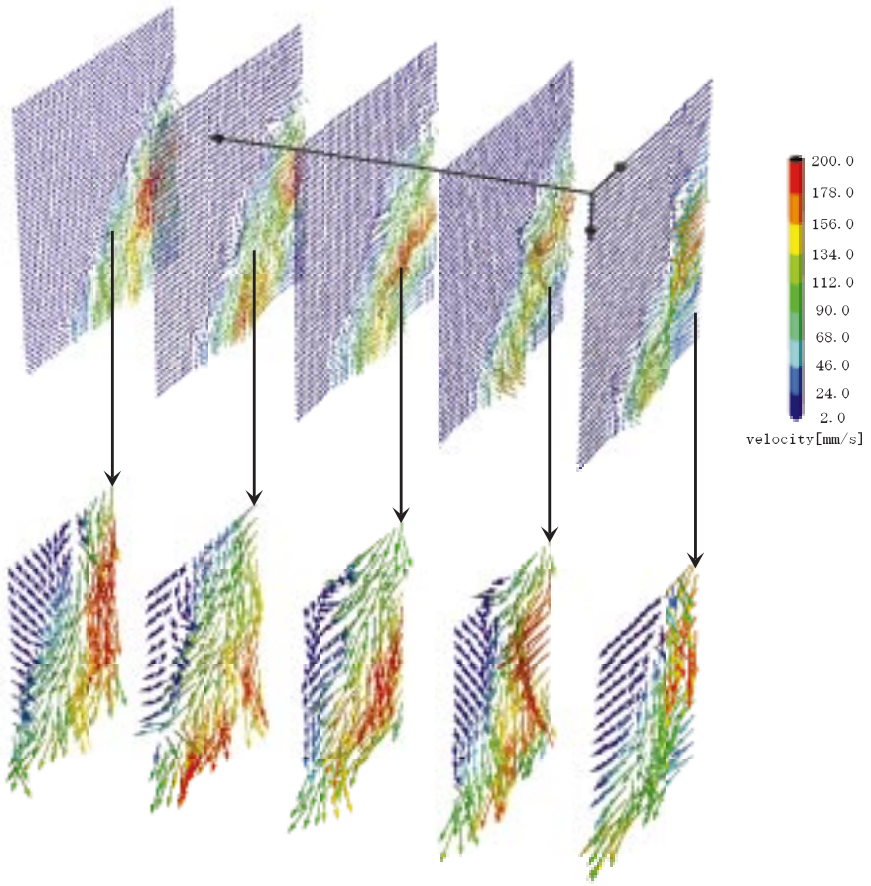

Figure 10 Sequence of SPIV velocity fields in (x, y) plane

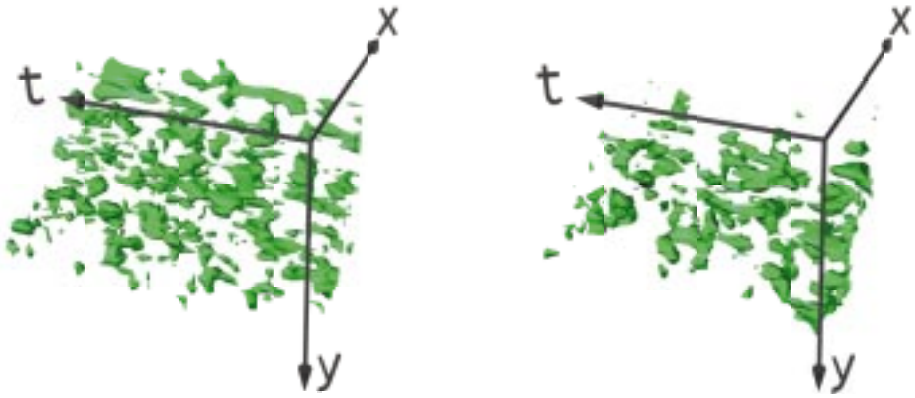

a) z=0 [mm] **b)** z=3 [mm]

Figure 11 Surfaces of constant vorticity magnitude ($|\omega_x| = 0.4|\omega_{x\max}|$)

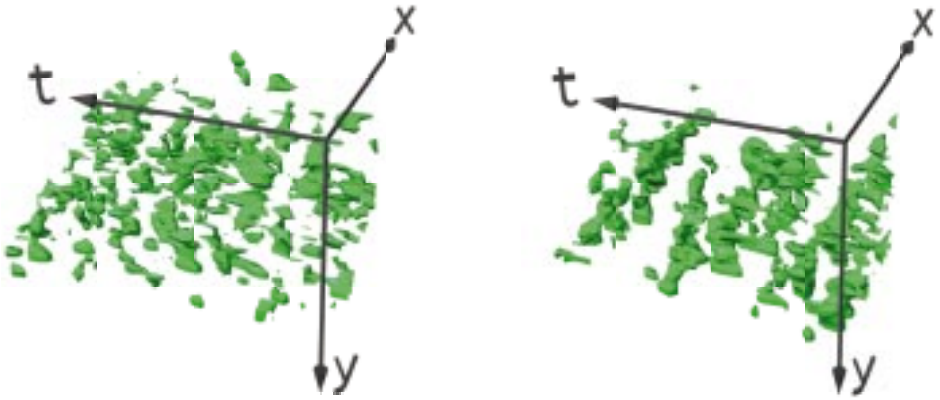

a) z=0 [mm] **b)** z=3 [mm]

Figure 12 Surfaces of constant vorticity magnitude ($|\omega_y| = 0.4|\omega_{y\max}|$)

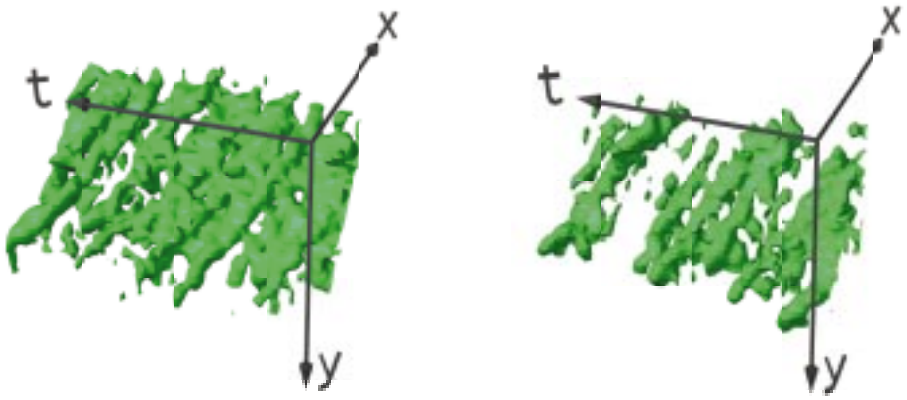

a) z=0 [mm] **b)** z=3 [mm]

Figure 13 Surfaces of constant vorticity magnitude ($|\omega_z| = 0.4|\omega_{z\max}|$)

5 Conclusions

A stereo PIV system was assembled, tested, and implemented in a two-dimensional flow case. The system was found to produce reliable and accurate measurements for mean in-plane and out-of-plane velocity when compared with classical PIV and LDV measurements. In part of the measurement plane, the SPIV system yielded rms velocities of out-of-plane that were overestimated. The out-of-plane error can be minimized by improving the calibration and transformation procedures. In this case the reliability of the measured in-plane velocity, as well as the limit in accuracy of the measured fluctuation of the final-conponent velocity was determined.

In addition the system was tested in a three-dimensional flow case. Owing to evaluation of the surfaces of constant vorticity magnitude distribution in the z-direction, three-dimensional vortical strucures were observed. The effect of a jet in a cross-flow in terms of mixing and the resultant velocity field is investigated using the SPIV system.

Acknowledgement

This work was supported by a Grant-in-Aid of the Japanese Ministry of Education, Science and Culture (grant No.10555062).

References

[1] Raffel M, Willert C E, and Kompenhans J, Particle Image Velocimetry, *Springer Verlag Berlin Heideberg*(1998)

[2] Prasad A K, and Adrian R J, Stereoscopic particle image velocimetry applied to liquid flows, *Exp. Fluids* **15**(1993), 49-60

[3] Soloff S M, Adrian R J, and Liu Z C, Distortion compensation for generalized stereoscopic particle image velocimetry, *Meas.Sci.Technol.* **8**(1997), 1441-1454

[4] Lawson N J, and Wu J, Three-dimensional particle image velocimetry: experimental error analysis of a digital angular stereoscopic system, *Meas.Sci.Technol.* **8**(1997), 1455-1464

[5] Willert C, Stereoscopic digital particle image velocimetry for application in wind tunnel flow, *Meas.Sci.Technol.* **8**(1997), 1465-1479

[6] Hart D P, The elimination of Correlation errors in PIV processing, *Proc. 9th Int. Symp. on Appl. of Laser Tech. to Fluid Mech.*, (Lisbon, July 13-16, 1998)

[7] Bjorkquist D C, Design and calibration of stereoscopic PIV system, *Proc. 9th Int. Symp. on Appl. of Laser Tech. to Fluid Mech.*, (Lisbon, July 13-16, 1998)

[8] Gogineni S, Goss L, and Roquemmore M, Manipulation of a jet in a cross flow, *Exp. Therm. Fluid Sci.* **16**(1998), 209-219

[9] Hishida K, and Sakakibara J, Combined PLIF-PIV technique for velocity/scalar fields, *Proc. 3rd Intl. Workshop on PIV'99*(Santa Barbara, September 16-18, 1999), 21-30

[10] Anderson S L, Khalitov D A, and Longmire E K, High spatial resolution stereoscopic PIV measurements in fully developed turbulent channel flow, *Proc. 3rd Intl. Workshop on PIV'99*(Santa Barbara, September 16-18, 1999), 95-106

[11] Abe M, Longmire E K, Hishida K, and Maeda M, A comparison of 2D and 3D PIV measurements in an oblique Jet, *Proc. 3rd Intl. Workshop on PIV'99*(Santa Barbara, September 16-18, 1999), 493-498